Proceedings Joint CHAMP / GRACE Science Team Meeting 2004

On the impact of baroclinic ocean dynamics on the Earth's gravity field

Maik Thomas and Henryk Dobslaw

Institute for Planetary Geodesy, Dresden University of Technology, Dresden, Germany

Abstract. By analysing real time model runs performed with the Ocean Model for Circulation and Tides (OMCT) with various forcing conditions, the impact of non-barotropic ocean dynamics on the time variable Earth's gravity field is estimated. The applied global ocean model is capable of simulating the three-dimensional thermohaline, wind- and pressure-driven circulation as well as lunisolar tidal dynamics and takes into account several so-called secondary effects, e.g., loading and self-attraction of a baroclinic water column, mass variations associated with sea-ice dynamics, and nonlinear interactions between tides and circulation which are commonly neglected in global numerical ocean models. In order to get insight into typical spatiotemporal patterns of ocean mass redistribution and consequently to identify oceanic regions of high impact on gravity changes, causative physical processes are separated and corresponding ocean bottom pressure fields reflecting the ocean's influence on the gravity field are analysed. Although monthly mean variabilities of ocean mass distributions are only slightly affected by loading and self-attraction and nonlinear interactions, instantaneously these secondary effects are responsible for anomalies in geoid heights up to about 1 mm, i.e., near the level of GRACE measurement noise. The baroclinic simulations suggest that ocean mass redistribution temporarily affect monthly mean gravity estimates obtained from GRACE down to horizontal scales of ~ 450 km.

Citation. Thomas, M., Dobslaw, H.: On the impact of baroclinic ocean dynamics on the Earth's gravity field, Proc. Joint CHAMP / GRACE Science Team Meet. 2004, published online, www.gfz-potsdam.de/pb1/JCG, 2005.

1 Introduction

Mass redistribution within and mass exchanges between the subsystems of the Earth are reflected by variations of global parameters of the Earth, e.g., rotational variations, the Earth's shape and gravity field. In principle, high precise sea surface heights from altimetry and gravity fields determined by the new satellite missions CHAMP, GRACE, and GOCE provide a measure of geophysical aspects of global change. However, gravity estimates directly obtained from satellite missions are restricted concerning resolution in time and in space, and these missions will alias non-resolved oceanic motions. Thus, additional methods from theory and modelling are necessary to eliminate non-resolved processes aliasing the mission results and, finally, to allow for interpretations of the high precise geodetic measurements. By means of numerical global ocean models it could be shown that ocean dynamics affect the recovery of the gravity field on subdaily up to seasonal time scales (e.g., Wahr et al., 1998, Wünsch et al., 2001).

The ocean model currently in use for dealiasing purposes during the GRACE gravity field estimation process is restricted to barotropic wind- and pressure-driven ocean dynamics and covers the global oceans from $75°$S to $65°$N (Hirose et al., 2001). Recently, Thompson et al. (2004) compared output from a barotropic and a baroclinic version of the Parallel Ocean Program (POP) model (Dukowicz and Smith, 1994) and concluded that using a barotropic model should be sufficient in reducing the high-frequency aliasing error caused by the oceans, since baroclinic oceanic variations are too slow to alias monthly gravity estimates. However, the baroclinic POP model applied by Thompson et al. (2004) as well as Wahr et al. (1998) exclusively accounts for thermohaline and wind-driven signals. In the following, additional contributions to short-term ocean mass variations caused by the pressure-driven circulation, secondary effects due to loading and self-attraction of a baroclinic water column, as well as nonlinear interactions between circulation and tides are estimated by means of numerical simulations with the Ocean Model for Circulation and Tides (OMCT).

Correspondence to: M. Thomas (maik.thomas@tu-dresden.de)

2 The numerical ocean model

In general, global ocean models can be classified in different ways: the models are either barotropic or baroclinic, they are free or constrained by data, and, traditionally, the models are pure tidal or general circulation models. In order to examine the validity of the conventional separation of circulation and tides in global models the Ocean Model for Circulation and Tides (OMCT) (Thomas et al, 2001; Thomas, 2002) was developed by adjusting the originally climatological Hamburg Ocean Primitive Equation Model (HOPE) (Wolff et al., 1996; Drijfhout et al., 1996) to the weather time-scale and coupling with an ephemeral tidal model. The model is based on the nonlinear balance equations for momentum, the continuity equation for an incompressible fluid and conservation equations for heat and salt. The hydrostatic as well as the Boussinesq approximations are applied. Implemented is a prognostic thermodynamic sea-ice model (Hibler, 1979) that predicts ice-thickness, compactness and drift. Prognostic variables are horizontal velocities, surface elevation, temperature, salinity, sea ice thickness and compactness. Higher order effects such as nonlinearities are accounted for as well as the secondary potential due to loading and self-attraction (LSA) of the water masses (see Thomas et al., 2001). Since baroclinic ocean models using the Boussinesq approximation conserve volume rather than mass and artificial mass and consequently bottom pressure changes are introduced due to applied heat and freshwater fluxes, following Greatbatch (1994) a spatially uniform layer is added to the sea-surface to enforce mass conservation (see, e.g., Ponte and Stammer, 2000; Gross et al., 2003). Considering the dominant diurnal and semidiurnal tides in a global general circulation model requires a significant increase of the time resolution. In the present configuration the model uses a time step of 30 minutes, a horizontal resolution of 1.875 degrees and 13 layers in the vertical.

In contrast to the traditional partial tide approach, the OMCT takes into account effects from the complete lunisolar tidal potential computed from the ephemerides of the tide-generating bodies. Initially, ephemerides were calculated during the model run by means of the analytical approach of van Flandern and Pulkkinen (1998) reaching accuracies of computed positions of about one arc minute which is sufficient in view of a grid resolution of 1.875°. Recently, these algorithms have been replaced by the more accurate ephemerides VSOP87 (Variations Seculaires des Orbites Planetaires) developed by Bretagnon and Francou (1988) to guarantee precise ephemerides over long periods (Hellmich, 2003). Thus, the model is now capable of generating precise ephemerides from knowledge of the actual date alone.

To estimate the quality of the tidal oscillation system produced by the ephemeris approach applied in OMCT, harmonic coefficients of main partial tides were extracted and contrasted to the ST103 data set of observed pelagic tidal coefficients according to Le Provost (1995). Although modelled tidal amplitudes are frequently about 10-20% lower than observed, phase differences are always below the level of significance, i.e., smaller than the time step applied (cf., Thomas, 2002). Despite comparatively coarse resolution in time and space, the ephemeris approach implemented in OMCT meets the quality of Seiler's (1991) free barotropic partial tidal model using a time step of 90 seconds and a horizontal resolution of 1 degree in latitude and longitude (Thomas and Sündermann, 1999). Naturally, a free model cannot be expected to meet the high quality of models constrained by observed data, e.g., by altimetry from TOPEX/POSEIDON. Thus, a consideration of 'free' tides in some simulations presented in the following is less intended for a reproduction of tidal observations as realistic as possible, but rather for estimations of effects that are generally not accounted for in standard models. In contrast to assimilated models, unconstrained models are physically consistent and allow additional fundamental investigations: Up to now, free models provide the only opportunity to estimate oceanic angular momentum caused by long-period tides on a global scale. The new concept of a free combined model of ephemeral tides and circulation realised in OMCT allows to estimate the mechanical impact of tidal dynamics on parameters of the general circulation, for instance on vertical mixing and therefore on the meridional overturning circulation. Further, the combined nonlinear model will reveal the importance of nonlinear interactions between partial tides as well as between tides and general circulation and, finally, the corresponding contributions to ocean mass redistribution. The latter are expected to be most pronounced on timescales where both tidal and circulation induced variations are significant, e.g., at seasonal timescales. According to Thomas et al. (2001), nonlinear interactions between tides and circulation and secondary effects arising from loading and self-attraction are responsible for about 8% of total oceanic excitation of polar motion on subseasonal to decadal timescales.

To produce a quasi steady-state thermohaline and wind-driven circulation, the OMCT was initially spun up for 265 years with cyclic boundary conditions, i.e., climatological wind stresses according to Hellerman and Rosenstein (1983) and annual mean surface temperatures and salinities according to Levitus (1982). The climatological initial model run was followed by a real-time simulation for the period 1958-2000 driven by wind stress components, 2m-temperatures, freshwater fluxes, and atmospheric surface pressure from the 40-year reanalysis project ERA-40 of the European Centre for Medium Range Weather Forecasts (ECMWF) covering the period from September 1957 to August 2002. The model results presented here are based on a subsequent OMCT run forced with operational atmospheric analysis data provided by ECMWF (see Dobslaw and Thomas, 2005). Both ERA-40 reanalyses and operational analyses have a time resolution of 6 hours.

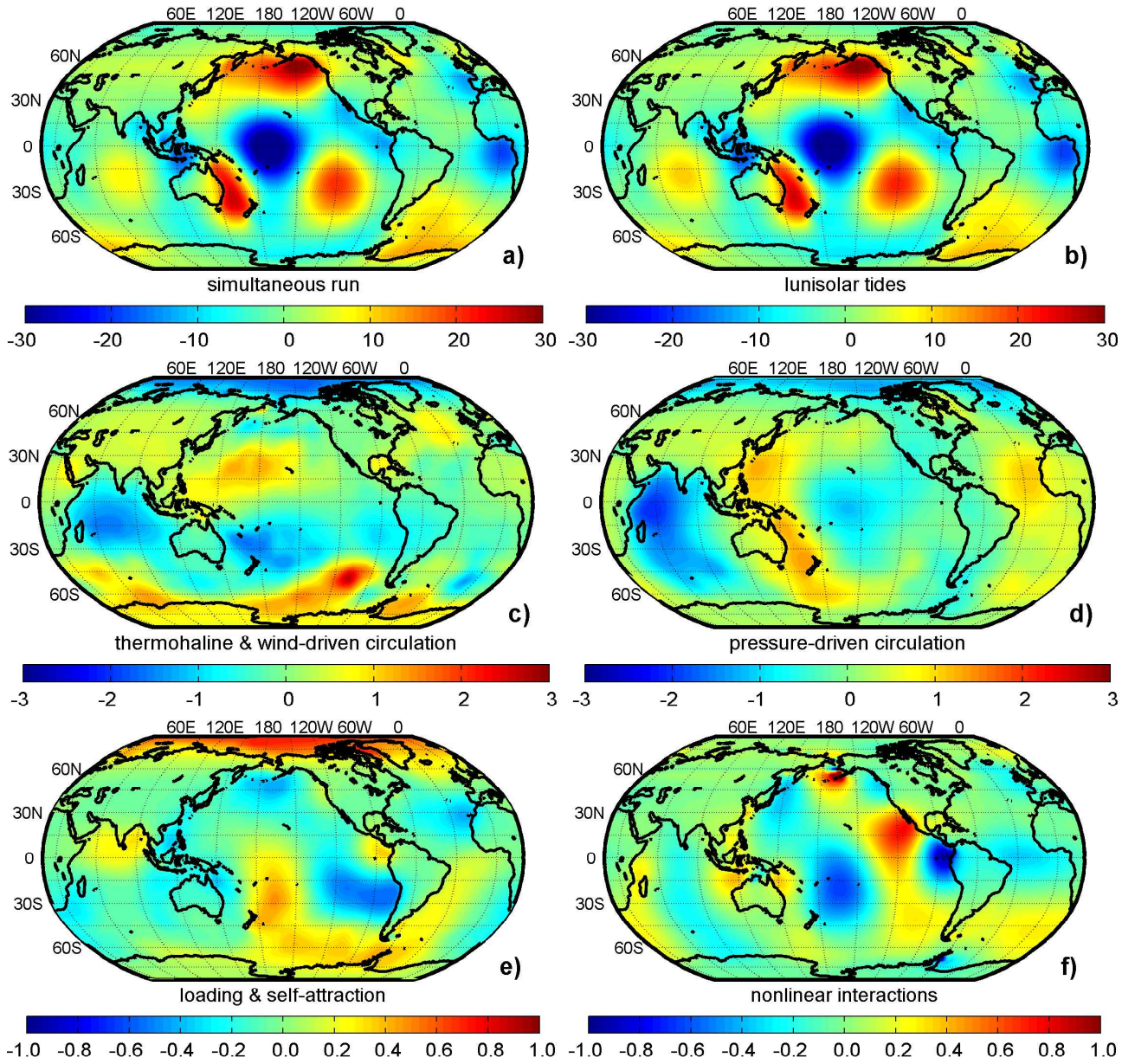

Fig. 1. Instantaneous ocean induced anomalies in geoid height in [mm] on 25 March 2004, 12:00 UTC: (a) simultaneous consideration of thermohaline, wind-, and pressure driven circulation and lunisolar tides including effects due to loading and self-attraction as well as nonlinear interactions; (b) contribution of lunisolar tides alone; (c) thermohaline and wind-driven circulation; (d) contributions due to deviations from a pure inverse barometric response of the sea surface to atmospheric pressure changes; (e) loading and self-attraction; (f) nonlinear interactions between general circulation and tidal dynamics.

3 Ocean induced geoid height anomalies

Ocean bottom pressure fields resulting from simulations driven with operational analysis data from ECMWF were expanded into time-dependent spherical harmonics up to degree $l = 100$, which is equivalent to a horizontal scale of about 200 km. The harmonic coefficients were transformed to variations in geoid height anomalies relative to the temporal mean of 2001 using Love loading numbers from Dong et al. (1996) for $l = 2 \ldots 9$ and from Farrell (1972) for $l = 10 \ldots 100$. In accordance with the GRACE solutions $l = 0, 1$ terms were not included. Exemplarily, in Fig. 1a an arbitrarily chosen snap-shot of the corresponding instantaneous distribution of geoid height anomalies resulting from a simultaneous model run of lunisolar tides and the thermohaline, wind-, and pressure driven circulation is given, including secondary effects arising from loading and self-attraction of a baroclinic water column and nonlinear interactions. Combined circulation and tidal induced anomalies are typically in the range of -3 to $+3$ cm. Not surprisingly, the dominant contribution is caused by lunisolar tides (Fig. 1b), whereas the sum of remaining influences of the thermoha-

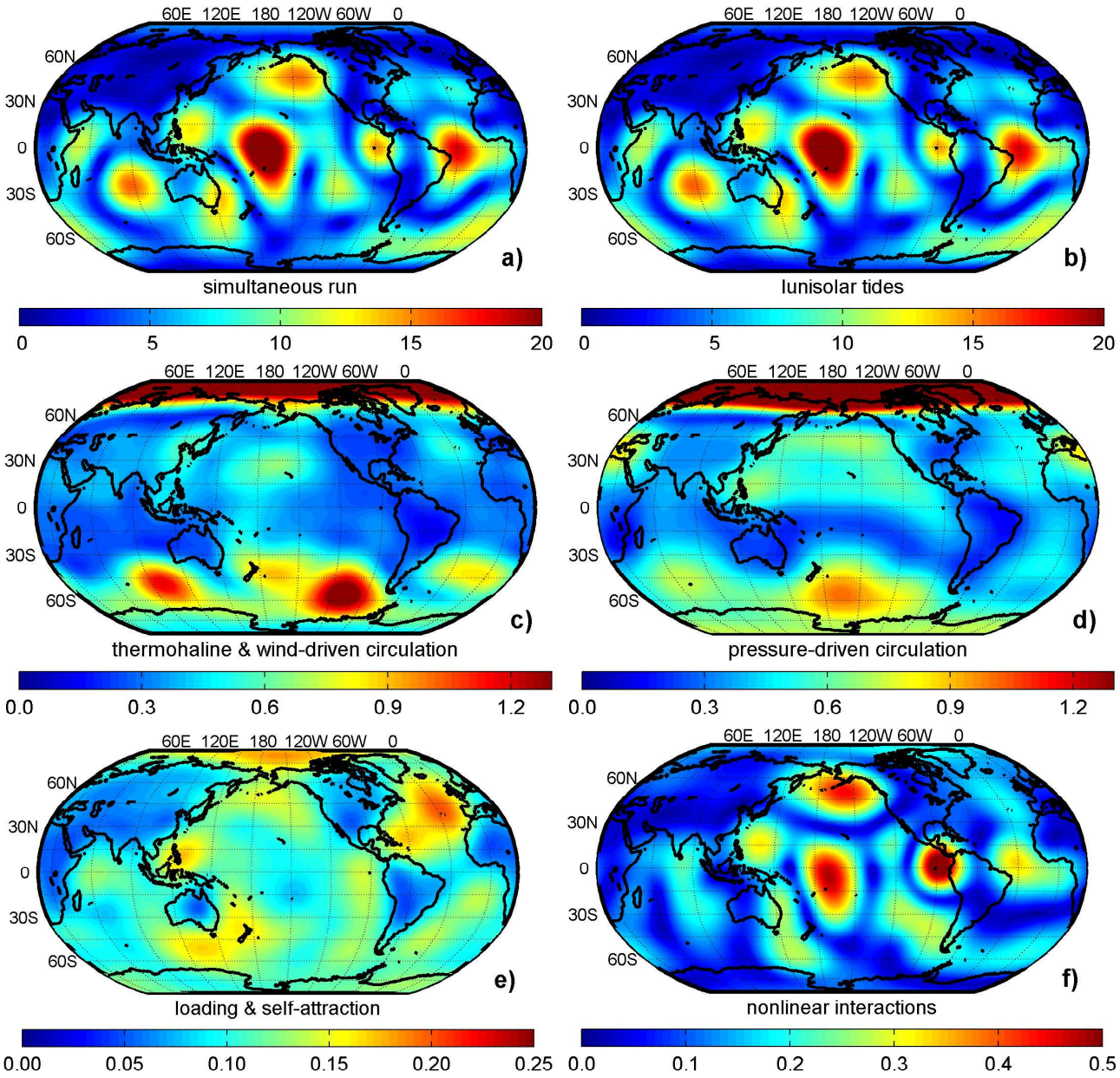

Fig. 2. Monthly rms-variability of geoid heights in [mm] in March 2004: (a) simultaneous consideration of thermohaline, wind-, and pressure driven circulation and lunisolar tides including effects due to loading and self-attraction as well as nonlinear interactions; (b) contribution of lunisolar tides alone; (c) thermohaline and wind-driven circulation; (d) contributions due to deviations from a pure inverse barometric response of the sea surface to atmospheric pressure changes; (e) loading and self-attraction; (f) nonlinear interactions between general circulation and tidal dynamics.

line, wind-, and pressure driven circulation as well as secondary effects is generally one order of magnitude smaller. According to Fig. 1c and 1d, circulation induced anomalies have to be mainly attributed to the thermohaline and wind-driven circulation; slightly minor contributions are caused by instantaneous deviations of the sea-surface from a purely inverse barometric response to atmospheric pressure changes. Secondary effects due to loading and self-attraction and nonlinear interactions between tides and general circulation generate additional geoid height anomalies with maximal amplitudes of about 1 mm (Fig. 1e and 1f).

To examine the influence of individual dynamical processes in the ocean on monthly mean gravity estimations directly obtained from satellite missions, distributions of monthly root mean square (rms) variabilities were calculated according to

$$rms(\phi,\lambda) = \sqrt{\frac{1}{K-1}\sum_{k=1}^{K}\left(N(t_k,\phi,\lambda) - \bar{N}(\phi,\lambda)\right)^2}\,, \quad (1)$$

where K is the number of calculated sets of spherical har-

monics per month, N the instantaneous and $\bar{N}$ the monthly mean geoid height anomaly at (ϕ, λ). As expected, the most important contribution to total ocean induced monthly mean geoid height variabilities seen in Fig. 2a are caused by tidal dynamics (Fig. 2b) reflecting the dominance of semi-diurnal and diurnal tides in submonthly ocean mass redistribution. As a consequence of the dominance of the lunar partial tide M_2 in the world ocean, obviously, the rms pattern is related to the well-known M_2 oscillation system. Again, about one order of magnitude lower amplitudes result from remaining influences of the general circulation with quite similar portions from the thermohaline and wind-driven circulation as well as pressure-driven circulation (Fig. 2c,d). High amplitudes around 1 mm are typically found in southern oceans associated with the Antarctic Circumpolar Current. Mean variabilities above 1.5 mm are generally located in the Arctic ocean due to the presence of sea-ice, since, for instance, in ice-covered regions an instantaneous invers-barometric response of the sea-surface is largely prevented. Though to less extent, according to Fig. 2e effects of sea-ice are also reflected in the variability pattern caused by loading and self-attraction. However, all in all the impact of loading and self-attraction on high frequency bottom pressure anomalies is rather small reaching maximal amplitudes of about 0.25 mm in the northeast Atlantic. As depicted in Fig. 2f, distinctly higher influences have to be attributed to nonlinear interactions between circulation and tides. Since phase velocities of the tidal waves depending on local water depths are modified in the simultaneous model run due to the actual sea surface topography resulting from the general circulation, contributions from nonlinear interactions are expected to be most pronounced where on the one hand the variability of tidal velocities and on the other hand circulation induced surface elevations are high. Thus, the rms-pattern of nonlinear effects resembles the tidal pattern shown in Fig. 2b particularly in Pacific regions where the mean surface topography is high, for instance, due to comparatively low salinities.

To analyse the spatial scales of ocean induced mass anomalies having an impact on satellite gravity estimations, degree variance spectra computed from daily, monthly, and annual differences of Stokes coefficients resulting from the combined effects of thermohaline, wind-, and pressure-driven circulation, loading and self-attraction, and nonlinear interactions are contrasted to (predicted) error spectra of the gravity missions. According to Fig. 3, annual oceanic signals are above the predicted error spectrum for GRACE up to degree $l = 42$, i.e., down to half-wavelengths of about 475 km. Compared to the results published by Wahr et al. (1998), who analysed output from the POP model, annual variabilities are slightly increased. This might be primarily attributed to the neglect of pressure forcing in the POP model as well as to distinctly different model characteristics.

While mean monthly ocean induced gravity anomalies as deduced from OMCT simulations are expected to affect GRACE gravity estimates up to degree $l = 39$ and consequently at spatial scales similar to annual signals, the required resolution for ocean dealiasing purposes drops to

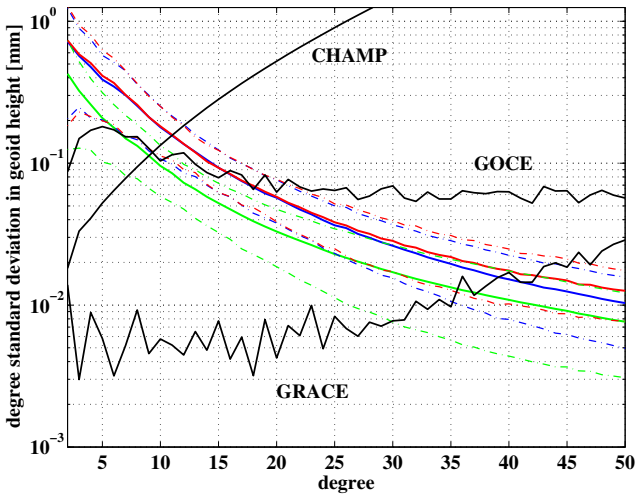

Fig. 3. Degree variance spectra of daily (green), monthly (blue), and annual (red) differences of simulated ocean induced geoid height anomalies (model year 2004). Solid lines represent mean spectra caused by the thermohaline, wind-, and pressure driven circulation considering loading and self-attraction as well as nonlinear interactions. Dash-dotted lines confine corresponding $2\sigma = 0.95$ confidence intervals. Black lines are predicted errors of the gravity missions.

$l = 35$ ($\sim$ 570 km) in the case of daily anomalies. Thus, daily anomalies are very similar to the results published by Wünsch et al. (2001) who analysed OMCT simulations forced with twice-daily climate model data from ECHAM3 simulations.

As expected, correlations of oceanic signals generally decrease with increasing time. However, confidence intervals at 2σ=0.95 (dotted lines in Fig. 3) show that these differences are highly variable, occasionally leading to significant annual and monthly variances up to degree $l = 45$ ($\sim$ 450 km). This value can be expected as a lower boundary for spatial resolution of ocean induced geoid height anomalies intended to be used for dealiasing purposes during the GRACE gravity field estimation process.

4 Conclusions

By means of numerical simulations with the Ocean Model for Circulation and Tides (OMCT) driven by 6-hourly atmospheric analysis data provided by ECMWF the impact of the thermohaline, wind-, and pressure driven circulation as well as secondary effects due to loading and self-attraction and nonlinear interactions between circulation and ephemeral tides on the temporal variable gravity field of the Earth have been estimated. According to rms variabilities exemplarily calculated for March 2004, monthly thermohaline and wind-driven signals cause geoid height anomalies exceeding 1 mm in several regions, particularly in the range of the Antarctic Circumpolar Current and in the Arctic Ocean. Similar monthly signals have to be expected from the pressure driven circulation with most pronounced contributions from

the Arctic Ocean, since due to the presence of sea-ice atmospheric pressure changes cannot be immediately compensated by deformations of the sea surface.

Since on the one hand an unconstrained model cannot compete with assimilated partial tide models, on the other hand the applied model has proven to reproduce tidal dynamics satisfactorily, here, we did not pay attention to the direct effect of ephemeral tides but focussed on secondary tidal effects and estimated the impact of nonlinear interactions between tidal dynamics and the general circulation on ocean mass distributions. Although corresponding monthly rms-values generally approach only 0.5 mm, these nonlinear contributions distinctly exceed the influences due to loading and self-attraction. Though mean variabilities are comparatively small, instantaneous anomalies caused by these secondary effects can reach the level of measurement noise, as indicated in Fig. 1.

Contrasting mean degree variance spectra calculated from simulated ocean induced geoid height anomalies to corresponding predicted error spectra of gravity missions suggests that ocean mass redistribution will have an impact on, for instance, monthly mean GRACE gravity fields at horizontal scales up to $\sim$ 510 km. However, simulated spectra themselves are characterised by high variances indicating that baroclinic oceanic signals temporarily affect GRACE gravity estimates up to degree $l = 45$, i.e., down to half wavelengths of about 450 km.

Acknowledgements. We thank the European Centre for Medium Range Weather Forecasts (ECMWF), Reading, UK, the Deutscher Wetterdienst, Offenbach, Germany, and the Deutsches Klimarechenzentrum, Hamburg, Germany for providing ECMWF ERA-40 and operational atmospheric analysis data. The OMCT simulations were performed on NEC SX6 of the Deutsches Klimarechenzentrum, Hamburg, Germany. This work was supported by the Deutsche Forschungsgemeinschaft under grant TH864/1-1.

References

Bretagnon, P., and Francou, G.: Planetary theories in rectangular and spherical variables. VSOP87 solutions, Astronomy and Astrophysics, 202, 309-315, 1988.

Dobslaw, H., Thomas, M.: Considering ECMWF forecast data for GRACE de-aliasing, Proc. Joint CHAMP / GRACE Science Team Meet. 2004, published online, www.gfz-potsdam.de/pb1/JCG, 2005.

Dong, D., Gross, R. S., and Dickey, J. O.: Seasonal variations of the Earth's gravitational field: an analysis of atmospheric pressure, ocean tidal, and surface water excitation, Geophys. Res. Lett., 23, 725-728, 1996.

Drijfhout, S., Heinze, C., Latif, M., and Maier-Reimer, E.: Mean circulation and internal variability in an ocean primitive equation model, J. Phys. Oceanogr., 26, 559-580, 1996.

Farrell, W. E.: Deformation of the Earth by surface loads, Rev. Geophys. Space Phys., 10, 761-797, 1972.

Greatbatch, R. J.: A note on the representation of steric sea level in models that conserve volume rather than mass, J. Geophys. Res., 99, 12767-12771, 1994.

Gross, R. S., Fukumori, I., Menemenlis, D.: Atmospheric and oceanic excitation of the Earth's wobbles during 1980-2000, J. Geophys. Res., 108(B8), 2370, doi: 10.1029/2002JB002143, 2003.

Hellerman, S., and Rosenstein, M.: Normal monthly wind stress over the world ocean with error estimates, J. Phys. Oceanogr., 13, 1093-1104, 1983.

Hellmich, A.-M.: Ein rechenökonomisches Modul für ephemeridische Gezeitensimulationen, Diploma Thesis, Techn. Univ. Dresden, Germany, 131pp., 2003.

Hibler III, W. D.: A dynamic thermodynamic sea ice model, J. Phys. Oceanogr., 9, 815-846, 1979.

Hirose, N., Fukumori, I., and Zlotnicki, V.: Modelling the high-frequency barotropic response of the ocean to atmospheric disturbances: Sensitivity to forcing, topography, and friction, J. Geophys. Res., 106, 30,987-30,995, 2001.

Le Provost, C.: A new sea truth data set for tides, ftp://meolipc.img.fr/pub/ST103, LEGI/IMC, BP 53X, 38041, Grenoble Cedex, 1995.

Levitus, S.: Climatological atlas of the world ocean, NOAA Professional Paper, 13, 173 pp., U.S. Department of Commerce, 1982.

Ponte, R. M, and Stammer, D.: Global and regional axial ocean angular momentum signals and length-of-day variations (1985-1996), J. Geophys. Res., 105, 17,161-17,171, 2000.

Seiler, U.: Periodic changes of the angular momentum budget due to the tides of the world ocean, J. Geophys. Res., 96, 10287-10300, 1991.

Thomas, M.: Ocean induced variations of Earth's rotation - Results from a simultaneous model of global circulation and tides, Ph.D. dissertation, University of Hamburg, Germany, 129 pp., 2002.

Thomas, M., and Sündermann, J.: Tides and tidal torques of the world ocean since the last glacial maximum, J. Geophys. Res., 104, 3159-3183, 1999.

Thomas, M., Sündermann, J., and Maier-Reimer, E.: Consideration of ocean tides in an OGCM and impacts on subseasonal to decadal polar motion excitation, Geophys. Res. Lett., 28, 12, 2457-2460, 2001.

Thompson, P. F., Bettadpur, S. V., and Tapley, B. D.: Impact of short period, non-tidal, temporal mass variability on GRACE gravity estimates, Geophys. Res. Lett., 31, L06619, doi: 10.1029/2003GL019285, 2004.

van Flandern, T. C., and Pulkkinen, K. F.: Low-precision formulae for planetary positions, The Astrophysical Journal-Supplement Series, 41, 3, Willmann-Bell Inc., 1998.

Wahr, J., Molenaar, M., and Bryan, F.: Time variability of the Earth's gravity field: Hydrological and oceanic effects and their possible detection using GRACE, J. Geophys. Res., 103, 30205–30229, 1998.

Wolff, J.O., Maier-Reimer, E., and Legutke, S.: The Hamburg Ocean Primitive Equation Model HOPE, Technical Report No. 13, 103 pp., DKRZ, Hamburg, 1996.

Wünsch, J., Thomas, M., and Gruber, T.: Simulation of oceanic bottom pressure for gravity space missions, Geophys. J. Int., 147, 428-434, 2001.